J Ther Eng, Vol. 9, No. 6, pp. 1531−1547, November, 2023

Journal of Thermal Engineering
Web page info: https://jten.yildiz.edu.tr
DOI: 10.18186/thermal.00000

Journal of Thermal Engineering

Research Article

# Heat transfer enhancement of electronic devices by using flexible printed circuit boards

**Mustafa EMAD[1], Sattar ALJABAIR[1,*], Ahmed Abdulnabi IMRAN[1]**

[1]*Department of Mechanical Engineering, Adana Alparslan Türkeş Science and Technology University, Adana, 01250, Türkiye*

## ARTICLE INFO

*Article history*
Received: 15 March 2022
Revised: 07 June 2022
Accepted: 11 June 2022

**Keywords:**
Flexible Printed Circuit Board;
Substrate Board Orientation;
Electronics System Cooling;
Enhancement Heat Transfer

## ABSTRACT

In this paper, heat transfer in electronic equipment was studied numerically and experimentally, by investing in the flexible printed circuit board and changing the board's orientation, which is the substrate of the electronic equipment from a vertical to a horizontal position. ANSYS Fluent software has been used to solve the continuity, momentum, and energy equations with the three-dimensional, unsteady, laminar and incompressible flow. In this study, the oscillatory motion equation was used as a boundary condition to represent the motion of the flexible board. In the experimental aspect of this study, a simulation of an ASUS motherboard (X399-A) with dimensions (30 x 25) cm and a Core i9 CPU with a fully working power of 130W was used to study the enhancement of heat transfer in the electronic devices by test rig specially made for this study. The results show that the flexible board's enhancement in the heat transfer was (7%) vertically and (7.6%) horizontally compared with the rigid board for the same working conditions. The horizontal position is better than the vertical of the two types of rigid and flexible board, with improved heat transfer rates of (2.7%) and (3%); correlation Equations of the Nusselt number from experimental results are presented.

**Cite this article as:** Emad M, Aljabair S, Imran AA. Heat transfer enhancement of electronic devices by using flexible printed circuit boards. J Ther Eng 2023;9(6):1531−1547.

## INTRODUCTION

Thermodynamic control is now an important consideration. Component downsizing and thermal system management have become more important as the electronic industry progresses. The majority of electronic equipment follows the same basic design, which considers the PCB board to be the electronic equipment's basis. Several researchers have explored heat transfer analysis in PCB. The efficiency of cooling electronic apparatuses was evaluated numerically by stressing the effects of various electronic component preparations [1]. It was shown that increasing the Ra number increases heat transmission greatly. The effect of varying processor power dissipation, fan speed, ambient air temperature, and air intake area on the (CPU) case temperature was investigated by [2]. Within the desktop computer equipment enclosure, the pattern of airflow and the optimum working temperature of different constituents were also identified.

Injection cooling studied directly a ball grid array as a source of heat generation [3]. It is proved through a case study that this integrative approach is an effective

***Corresponding author.**
*E-mail address: Sattar.J.Aljabair@uotechnology.edu.iq

*This paper was recommended for publication in revised form by Regional Editor Prof. Dr. Ahmet Selim Dalkilic*

Published by Yıldız Technical University Press, İstanbul, Turkey

methodology that leads to innovative design. A novel, enhanced, and highly integrated cooling technique is given for electronic packaging for a variety of steady-state operating conditions. Heat dissipation paths, both active and passive are being studied by [4]. A novel component layout integrating passive pathways and leveraging the backside of the liquid crystal display screen was presented as a result of the findings and a simple correlation-based thermal analysis of the proposed system. Heat dissipation rate from heat sources was investigated by placing them at the bottom of the PCB and comparing all heat source cooling techniques. It was determined that mixed convection is a better way for cooling discrete heating elements than free convection [5]. A design approach investigated of deflection, and stress in flexible printed circuit boards. To find out how the newly proposed FPC motherboard behaves under fan flow circumstances in a PC case, the intake and the systems of the two propellers had a considerable influence on the amount of deflection and stress, according to the findings of this study [6]. Numerical study of the wall temperature of an internally finned tube by solving Navier–Stokes equations using fluent software for a steady-state and laminar flow of fluid inside a tube under mixed flow conditions [7]. The study found that triangular-shaped fins had the lowest wall temperature compared to rectangular and T-shaped fins. CFD tool used to calculate the effects of different parameters and variation in heat flux distribution of the elements on the average Nusselt number and heat transfer coefficient in two-dimensional ribbed channels [8]. Numerical study of natural convection inside a two-dimensional rectangular cavity with a triangular ceiling and an adiabatic solid strip added in the cavity's center presented by [9]. The study was done using the finite volume method. This research aims to take a look at the fluid flow pattern and heat transport phenomena that occur when a solid strip is inside a rectangular hollow. Level electronic packaging of apparatus in the thermal design were investigated and confirmed by [10]. The application of CFD to the thermal design of complex electronics regimes yielded significant results. Unsteady analysis of a heated inclined finplate investigated at a 45º angle by using ANSYS FLUENT [11]. The findings of this study are utilized to look into heat transmission from the finned plate to the environment. Airflow rate and heat effects presented on an FPCB with an attached ball grid array (BGA) package [12]. The results revealed that the Reynold numbers and heat have a substantial impact on the deflection and stress of the FPCB. As a result, when dealing with the FPCB underflow scenario, it was critical to consider the temperature effect. It was discovered that the Nusselt number has a strong relationship between the geometric factors and the flow velocity. At a constant heat flow of 1000 $Wm^{-2}$ and atmospheric natural convection conditions, the cooling of a plate (1 m in height and 1 m in width) is oriented vertically, as well as 20° and 45° inclined from the vertical (downward-facing surface) was investigated by [13]. The findings show that the surface temperature values of the plate with an inclination angle of 45° are higher than those of the plate in its upright state and those of the plate with an inclination angle of 20° angle. Nadooshan et al. Numerical simulation of a three-dimensional incompressible laminar flow heated array of circular perforated fins studied by [14]. The SIMPLE algorithm was used to solve Navier–Stokes and energy equations using a finite volume technique. Calculations were carried out for Re numbers ranging from 100 to 350. The thermal performance, effectiveness of perforated, solid fins and their friction coefficient are determined. The results reveal that when the Re numbers and the number of holes increase, the average coefficient of friction decreases. The rate of H.T increases as the porosity and Reynold numbers increase. Mathew et al. [15] studied the (IC) chips provided with various heat fluxes subjected to the laminar forced convection. The goal is to cool the (IC) chips by choosing the best location, inclination angle, and size. Thermal and structural mechanics investigated by [16]. Where the study provides future PCB optimal design recommendations and a heat dissipation mode option in circuit board simulation. Salah et al. [17] studied the influence of heat flux, Re numbers, and baffle layout on H.T and flow behavior inside the enclosure. The results reveal that increasing the baffle width has no discernible effect on H.T, and that partially cut baffles provide a 30 per cent improvement over the plain heating block. At Re = 0 and q = 240 w/$m^2$, the baffle cases reduce the block surface temperature by roughly 11 per cent compared to the plain case. Numerical investigation performed on laminar forced convection air cooling of high thermal conductivity printed circuit boards with Single and multilayer copper sheets, which are used as substrate materials [18]. The heat transmission rate from the multi-layered copper-covered board is encouraging compared to a single-layer equivalent. Mehta et al. [19] investigated various operational aspects (charge ratio, orientation, and heat load) and the geometrical characteristics of a closed-loop flat-plate oscillating heat pipe, using acetone as the working fluid. Operational and geometrical features were shown to impact the thermal resistance measured significantly. heat transmission in a computer studied by [20]. They discovered that altering the airflow rate boosted heat transfer and helped satisfy the required cooling environment for the safe operation of electronic components. A development model investigated that defines a printed circuit board's power dissipation procedure [21]. It was built on well-known physical relationships and the finite difference method (FDM). According to the findings, the developed model can be used to precisely analyze the thermal regime of electronic equipment. Bilawane et al. [22] investigated natural convection by determining the heat transfer coefficient on plain, semi-roughed, and roughed plates. From a plain to a semi-roughed plate, the heat transfer coefficient increased by 6.63 per cent, 3.87 per cent from a semi-roughed to a roughed plate, and 10.75 per cent from a plain to a roughed plate at the ultimate heat input. Intensive study on heat transport in electronic circuits, a categorization of existing cooling technologies, and an investigation into the use of the FPCB in

electronic equipment presented by [23]. Dash et al. [24] conducted an extensive study to improve the microchannel's thermal efficiency. In this work, the available investigations and results have been thoroughly examined in order to provide a clear roadmap for future study into channel geometry selection. The use of a flexible board to replace a rigid board was investigated to take advantage of the board's oscillation feature to enhance heat transfer straight through the board. This means using advanced heat transfer technologies to reduce the temperature of electrical equipment and reduce energy consumption for cooling electronic devices is environmentally friendly by being a recyclable material as show in Figure 1. In the current study, the heat transmission of a model of the motherboard (ASUS X399-A) was investigated numerically and experimentally. A numerical study includes solving the continuity, momentum, and energy equations by

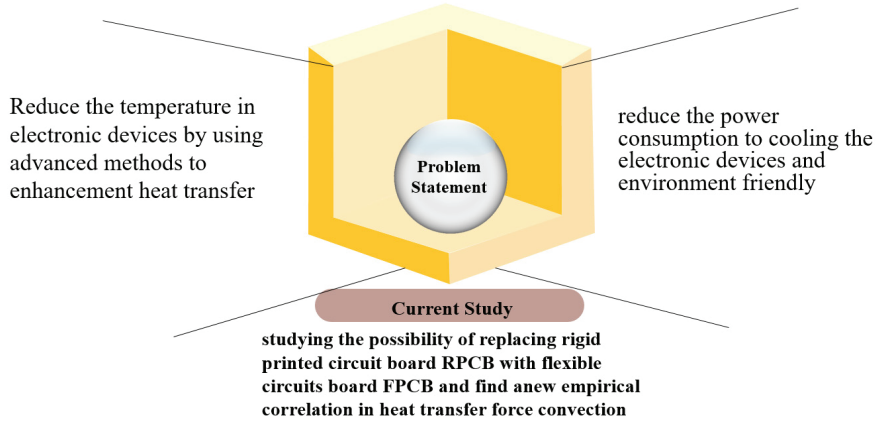


**Figure 1.** Problem statement of the current case study.

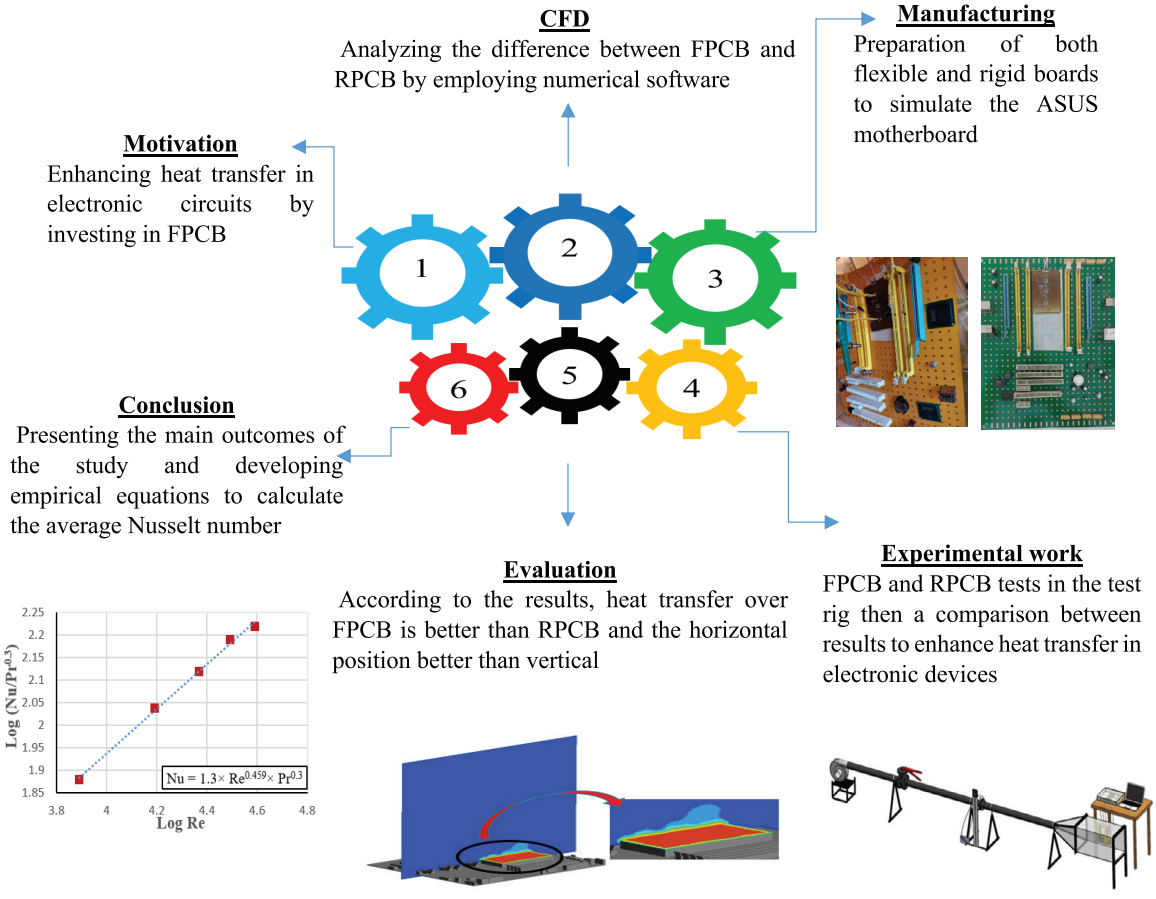


**Figure 2.** Main steps of the present study.

using analysis software when it was under laminar single-phase incompressible flow with various Reynold numbers (7000-40000). In experimental work, the ASUS X399-A motherboard with Core i9 CPU at the power of 130 W was simulated using both a flexible and rigid board, as shown in figure 2. Then, the numerical results are analyzed and compared with the experimental results.

## NUMERICAL METHOD

### Physical Domain

CFD was used to investigate the flow and temperature field distribution on the motherboard computer mounted in the test section to analyze the motherboard's thermal and hydraulic properties. A three-dimensional solid-fluid coupled model was employed with a finite volume CFD-based technique and a saleable solver to estimate the behavior of flow as well as heat transmission. The schematic motherboard dimensions are (30×25) cm×1 mm thickness as shown in Figure 3 (A) and the test section length is 800 mm, as illustrated in Figure 3 (B) for a rectangular channel with a square cross-section of 400 mm×400 mm.

### Governing Equations and Formulation

The present study considers air flow that is laminar, single-phase, and incompressible, as well as an unsteady-state process for flexible printed circuit boards and a steady-state procedure for rigid boards. Also included are the three-dimensional continuity, momentum, and energy equations. With the above-mentioned assumptions, the governing equations for this conjugated heat transport problem are as follows [25, 26]:

Continuity equation

$$\frac{\partial u}{\partial x}+\frac{\partial v}{\partial y}+\frac{\partial w}{\partial z}=0 \quad (1)$$

Momentum equation

$$\frac{\partial u}{\partial t}+u\frac{\partial u}{\partial x}+v\frac{\partial u}{\partial y}+w\frac{\partial u}{\partial z}=-\frac{1}{\rho}\frac{\partial p}{\partial x}+v\left(\frac{\partial^2 u}{\partial x^2}+\frac{\partial^2 u}{\partial y^2}+\frac{\partial^2 u}{\partial z^2}\right) \quad (2)$$

$$\frac{\partial v}{\partial t}+u\frac{\partial v}{\partial x}+v\frac{\partial v}{\partial y}+w\frac{\partial v}{\partial z}=-\frac{1}{\rho}\frac{\partial p}{\partial y}+v\left(\frac{\partial^2 v}{\partial x^2}+\frac{\partial^2 v}{\partial y^2}+\frac{\partial^2 v}{\partial z^2}\right) \quad (3)$$

$$\frac{\partial w}{\partial t}+u\frac{\partial w}{\partial x}+v\frac{\partial w}{\partial y}+w\frac{\partial w}{\partial z}=-\frac{1}{\rho}\frac{\partial p}{\partial z}+v\left(\frac{\partial^2 w}{\partial x^2}+\frac{\partial^2 w}{\partial y^2}+\frac{\partial^2 w}{\partial z^2}\right) \quad (4)$$

Where ρ, $p$ and ν are the density, pressure drop and kinematic viscosity of the coolant, respectively.

The fluid's energy equation is:

$$\rho Cp\left(\frac{\partial T}{\partial t}+u\frac{\partial T}{\partial x}+v\frac{\partial T}{\partial y}+w\frac{\partial T}{\partial z}\right)=-k\left(\frac{\partial^2 T}{\partial x^2}+\frac{\partial^2 T}{\partial y^2}+\frac{\partial^2 T}{\partial z^2}\right) \quad (5)$$

### Boundary Conditions

The model gets its inputs from the boundary conditions defined in the processor. Figure 3 b depicts the fluid and solid domains and also boundary conditions. The following boundary conditions are given for the computing zone:

- Test suction inlet

Velocity of the uniform flow is assumed $U_{in}$ = (0.5 →2.5) m/s

Air temperature Tin = 30°C

- Test section outlet $p_{out}$ = atmosphere pressure.
- All channel walls have no-slip wall U = V = W = 0.
- The CPU wall surface is exposed to a constant heat flux of 37142 W/m² [2, 27] and the other walls are adiabatic.

In this case study, transient flexible board motion is used in numerical simulation situations to reduce calculation instability. The flexible board moves at a constant speed in each case, and the location varies in each time step

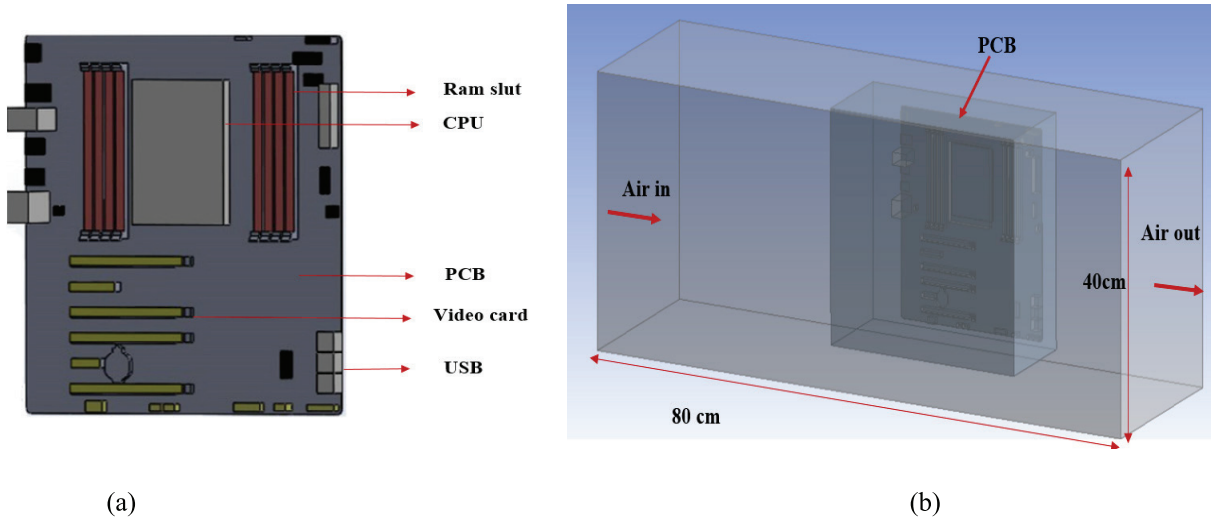


**Figure 3.** a) Schematic Asus motherboard (X399-A) for current case study b) Fluid domain.

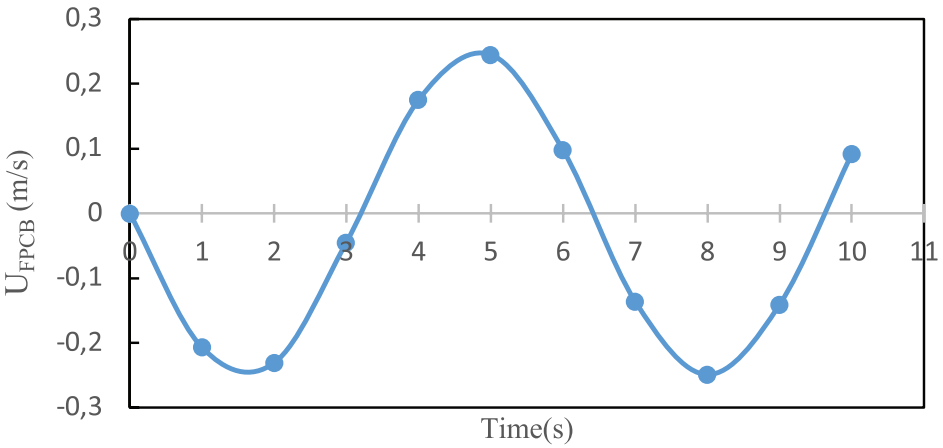


**Figure 4.** Fluctuation movement of the flexible motherboard and CPU for 10 second.

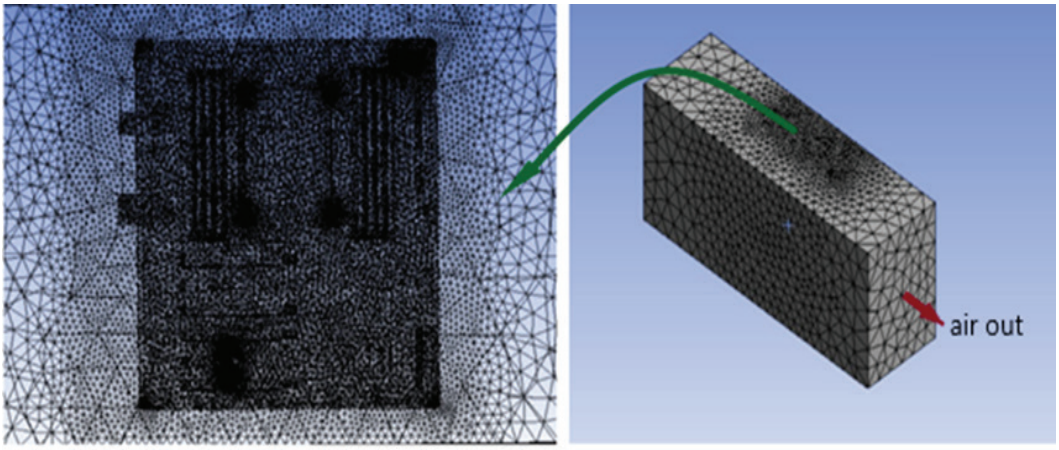


**Figure 5.** Mesh generation for motherboard and test section.

dependent on the board's position in the domain, as shown in figure 4. The UDF source file is compiled and built in a shared library for the created objects [28].

- Flexible motherboard and CPU fluctuation movement = UFPCB= 0.25 ×sin (t×1 /0.06×22/7).

**Grid Generation**

Structured meshes were used in the inlet and exit, as well as the channel, in the test section. To appropriately anticipate temperature and velocity gradients, the meshing was directed around the motherboard into the boundary layer region. The mesh creation for the test portion is shown in Figure 5. The number of nodes, in this case, was 3934547, while the number of elements was 2896726. A calculator with an Intel(R) Core (TM) i7-9750H CPU running at 2.60GHz and 2.59 GHz and 16.0 GB of RAM was used for this project.

**Grid Independency**

As demonstrated in figure 6, the phrase "grid independence" refers to improving efficiency by doing computations with lower cell sizes to arrive at the proper answer, resulting in a smaller mesh. Starting with a coarse mesh and gradually developing it until the changes in the data observed are less than a pre-determined suitable error is the typical CFD procedure.

## EXPERIMENTAL PROCEDURE

Figure 7 shows the main steps in this work, which include manufacturing the device, calibrating the measuring equipment, preparing a model of the rigid and flexible board, operating the system to reach a stable state, and then recording the results. Figures 8 and 9 show the main components of the device. The test section was built from a box made of an iron frame with a thickness of 2 mm, covered with transparent plastic glass with a thickness of 6 mm. RPCB and FPCB are used to simulate a real ASUS X399-A motherboard. During the experiment, a gate valve was used to control the flow volume in order to regulate the

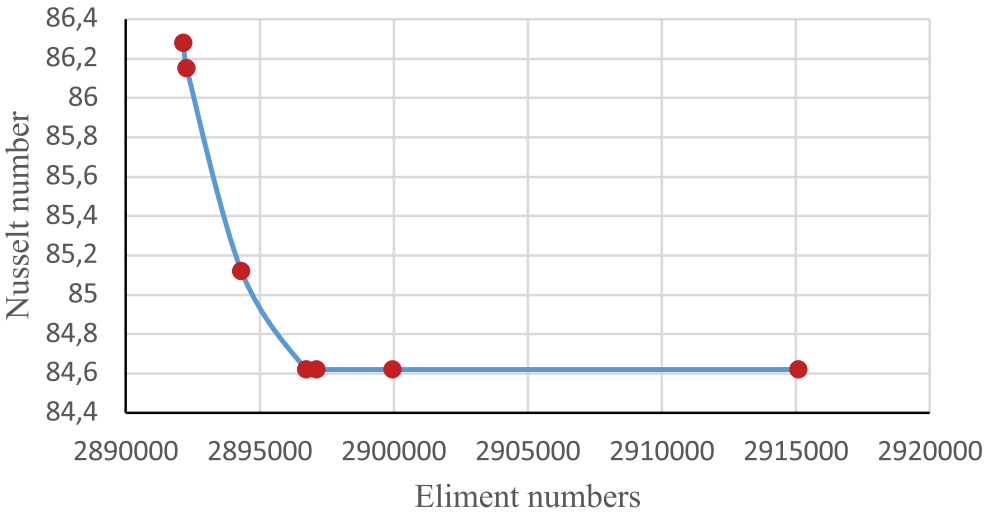


**Figure 6.** Grid Independency test for current case study.

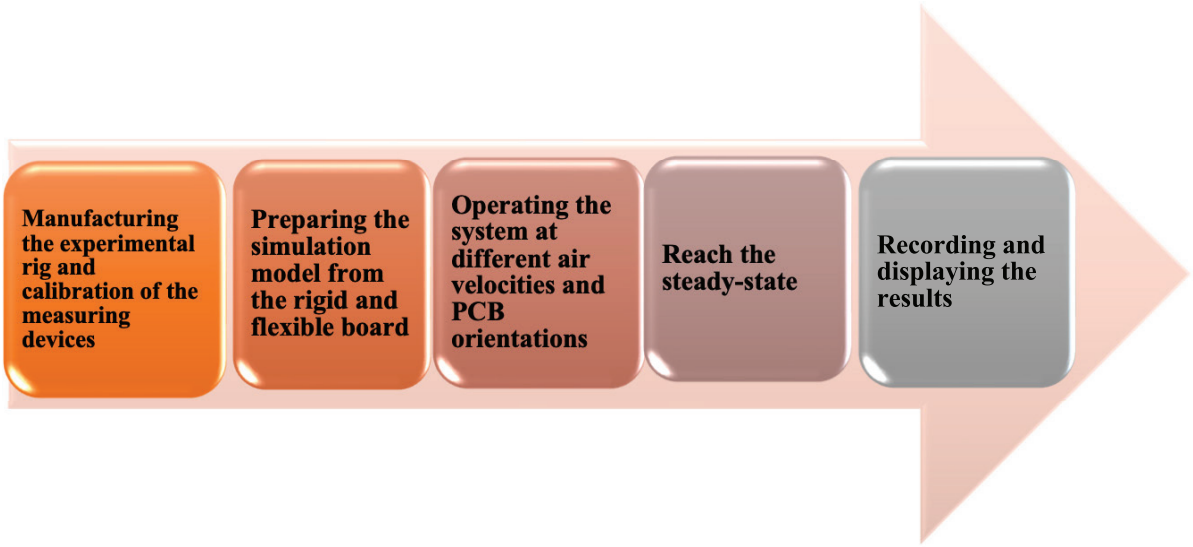


**Figure 7.** Diagram for experimental project steps.

**Figure 8.** Photograph of the experimental rig.

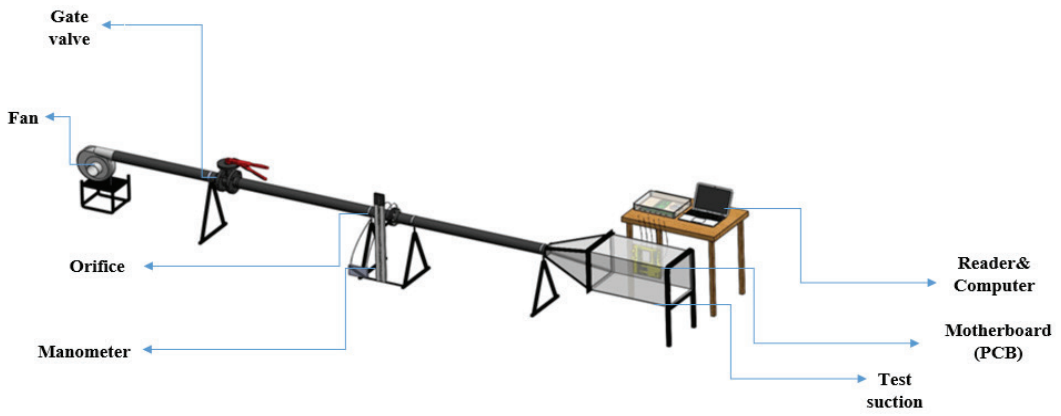


**Figure 9.** Schematic diagram for experimental rig.

flow velocity. An orifice plate was used to measure the flow volume in order to control the flow velocity in the range of 0.5 to 2.5 $m^2$/sec. An electric heater with thermal power of 130 W [2, 27] in the 35 $cm^2$ range was used to determine the CPU as a heat source in the motherboard. A multimeter was used to determine electrical energy by measuring electric current and voltage. To reach the intended power, power regulation was achieved by modulating the voltage source. Four K-type thermocouples were placed equally spaced in the CPU, and one at the input and output of the test area, as shown in Figure 10. The thermocouples were connected to the Arduino Mega 2560, and the data was sent to a computer for display and recording. The thermal heat transfer coefficient, Reynolds number, and Nusselt number are calculated as shown below. If the inlet air temperature is the same as the ambient temperature, it is used as the reference temperature.

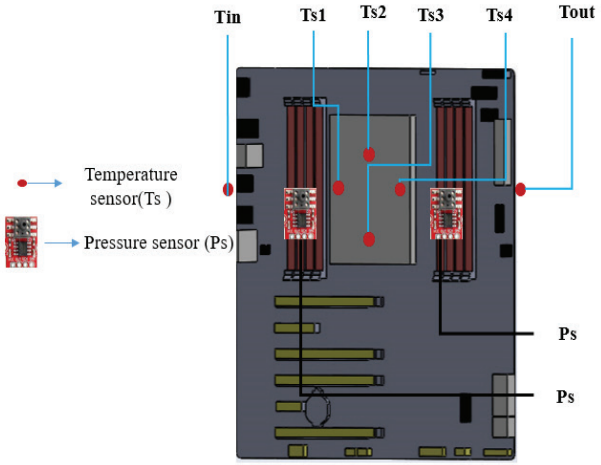


**Figure 10.** Sensor's locations.

**Table 1.** Experimental data reduction

| Variables | Equations |
|---|---|
| heat flux on the CPU outer surface | Q= IV |
| Average heat transfer coefficient | $h_{avg} = \frac{Q}{A(T_s - T_b)}$ |
| The mean bulk fluid temperature | $T_b = \frac{To+Tin}{2}$ |
| characteristic length | $lc = \frac{4A}{P}$ |
| The average Nusselt number | $Nu_{avg} = \frac{h_{avg} \quad lc}{k}$ |
| Reynold Number | $Re = \frac{\rho \times U_2 \times lc}{\mu}$ |
| Friction Factor | $f = \frac{2\,\Delta pD}{l\,\rho U^2_2}$ |

## UNCERTAINTY ANALYSIS

Because of measurement instrument error, the quantities used to determine the Nusselt number are subject to some uncertainty [29]. The experiment's uncertainties were assessed using the independent parameters measured in the experiments: voltage, current, and (inlet, outlet, and CPU) temperatures, as shown in Figure11.

### The Nusselt Number

The result *R* is generally calculated in some way from the *Xi* data.

*R= R(X1, X2..... Xi)*

$$\delta RXi = \frac{\partial R}{\partial Xi} \times \delta Xi$$

$$\delta R = \left[\sum_{i=1}^{M} \left(\frac{\partial R}{\partial Xi} \times \delta Xi\right)^2\right]^{\frac{1}{2}}$$

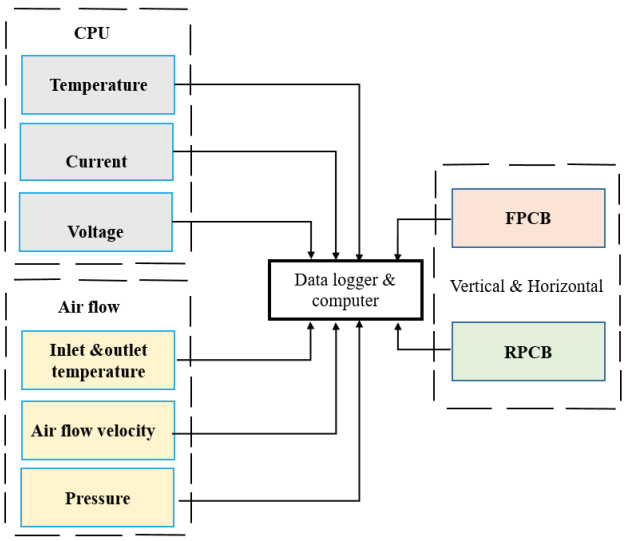


**Figure 11.** Measuring system diagram for experimental study.

The uncertainty interval (S) in the result can be given as:

$$S_R = [(Rx1Sx1)^2 + (Rx2Sx2)^2 + \cdots (Rxi\ Sxi)\ 2]^{0.5}$$

In dimensionless form:

$$\frac{SR}{R} = \left[\left(\frac{\partial R}{\partial X1}SX1 + \frac{\partial R}{\partial X2}SX2 \ + \cdots \frac{\partial R}{\partial Xi}SXi\right)^2\right]^{0.5}$$

$$RXi = \frac{\partial R}{\partial Xi}$$

$$Nu = \frac{hl}{k}$$

At Reynold = 7778, ΔT=44, I (amp) = 0.6A, V (volt) = 220 V

$$h = \frac{Q}{A\Delta T}$$

$$Nu = \frac{IVL}{A\Delta Tk}$$

$$\frac{\partial Nu}{\partial I} = \frac{Vl}{A\Delta Tk} = \frac{220\times0.05}{0.075\times44\times0.02588} = 128.7$$

$$\frac{\partial Nu}{\partial V} = \frac{I\,l}{A\Delta Tk} = \frac{0.6\times0.05}{0.075\times44\times0.02588} = 0.35$$

$$\frac{\partial Nu}{\partial \Delta T} = \frac{IV\,l}{A\Delta T^2 k} = \frac{0.6\times220\times0.05}{0.075\times44^2\times0.02588} = 1.75$$

The uncertainty Nusselt Number will be as in this equation:-

$$S_{Nu} = \left[\left(\frac{\partial Nu}{\partial I}si\right)^2 + \left(\frac{\partial Nu}{\partial V}sv\right)^2 + \left(\frac{\partial Nu}{\partial \Delta T}s\Delta T\right)^2\right]^{0.5}$$

$$si = \frac{\pm0.1}{0.6} = 0.16$$

$$sv = \frac{\pm0.1}{220} = 4.5\times10^{-4}$$

$$s\Delta T = \frac{\pm0.25}{220} = 1.1\times10^{-3}$$

$$S_{Nu} = [(128.7\times0.16)^2 + (0.35\times4.5\times10^{-4})^2 + (1.1\times10^{-3}\times1.75)^2]^{0.5} = \pm20.6\%$$

$$\text{Relative error} = \frac{SNu}{Nu} \rightarrow \frac{0.206}{70} = 0.003$$

## RESULTS AND DISCUSSION

### Flow Effect on Heat Transfer in Printed Circuit Board

#### Rigid printed circuit board

Since the motherboard is cooled by forced convection, the flow speed has an important effect on heat transfer. The average Nusselt numbers will rise and the motherboard temperature will decrease. Figure 12 shows the relationship between the average Nusselt numbers and the various Reynold numbers (7000 - 40000), an increase in the air velocity over the motherboard will increase the heat transfer coefficient because of an increase in a temperature difference ($\Delta T$) between the air and motherboard [2, 10, 30]. The results of the numerical study showed good agreement with the experimental study with the error rate in the vertical position (2.8%), and in the horizontal position (2.7) % respectively.

#### Flexible printed circuit board

In the flexible board, the heat transfer is studied in the same conditions as the previous work. The results show in Figure 13 that the procedure correspond to an increase in the average Nusselt number at ten-second with increasing the Reynold number in the horizontal and vertical positions with differences between the numerical and

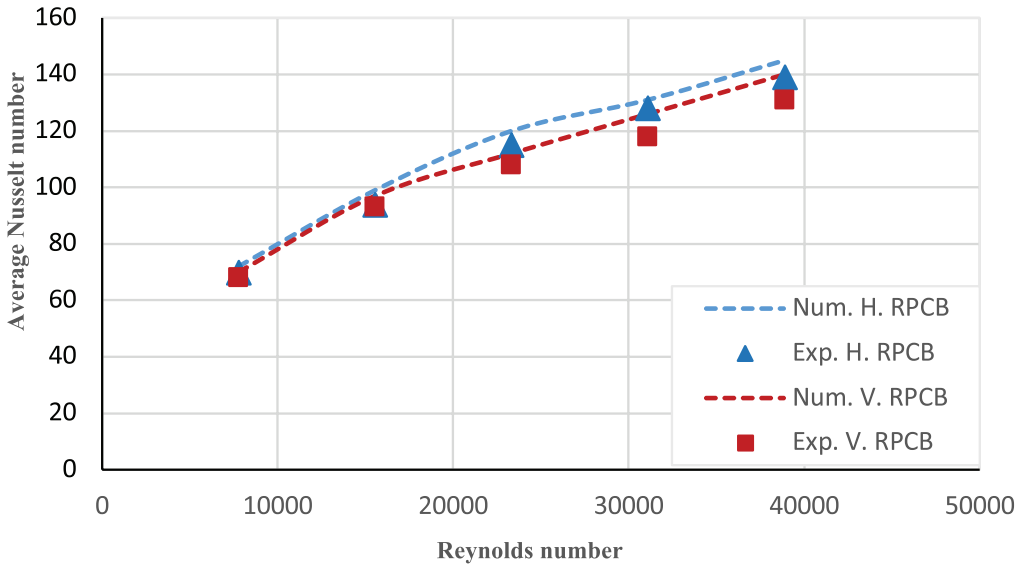


**Figure 12.** Comparison results between Experimental and numerical rigid printed circuit board with a variation of average Nusselt number numbers with Reynolds numbers at a different orientation.

experimental solution (3.4%) vertically and (2.6%) horizontally. The heat transfer of the flexible board is better than the heat transfer of the rigid board as shown in Figures 13 and 14 the percentage of improvement in average Nusselt number numbers is (7.6%) in the horizontal position and (7%) in the vertical position. The rise in air velocity causes an increase in vibration frequency, which causes a rapid change in the thickness of both hydrodynamic and thermal boundaries, as well as acting as a quick slack breaker layer. As a result, heat transmission between the turbulent bulk flow and the boundary layers is extremely efficient, resulting in a considerable increase in the heat transfer coefficient. [31, 32].

**Orientation Effect on Heat Transfer in Printed Circuit Board**

The average Nusselt number in the vertical position of the rigid and flexible printed circuit board is smaller than that for the horizontal counterpart as shown in Figures 14 and 15 because the buoyant force acts to generate secondary currents that are formed and moved in an upward perpendicular direction to the direction of flow in the vertical rigid and flexible printed circuit board, and there is recirculation

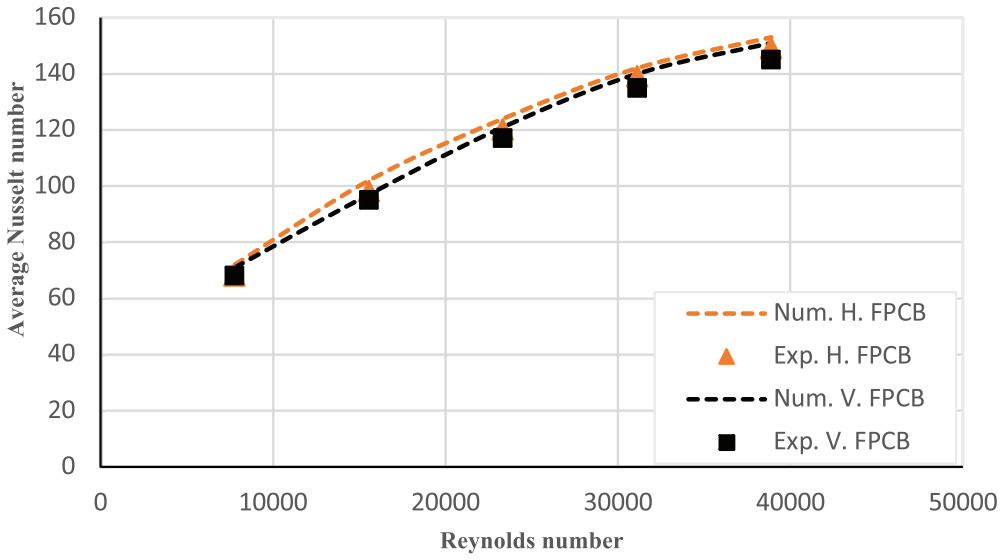


**Figure 13.** Comparison results between Experimental and Numerical flexible printed circuit board with a variation of average Nusselt numbers with Reynolds numbers at a different orientation.

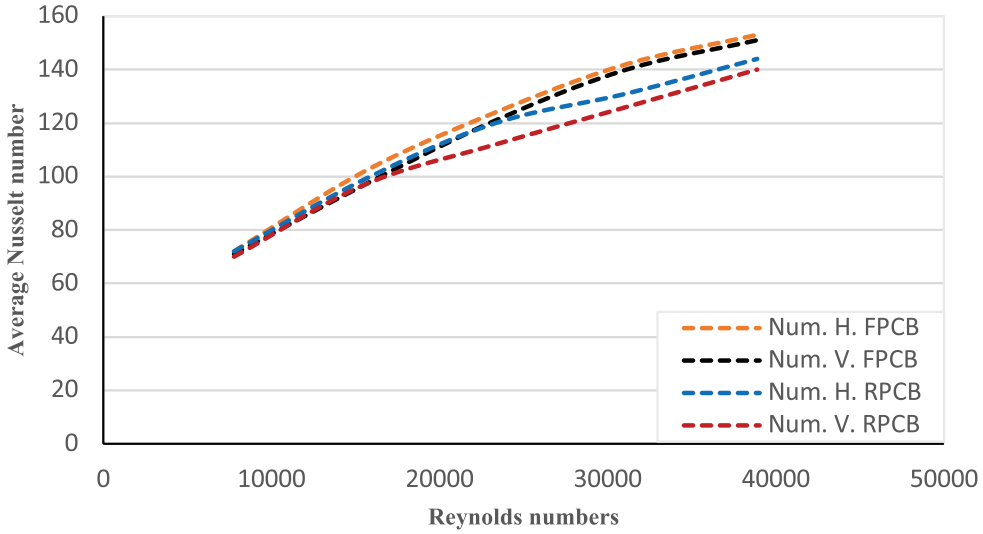


**Figure 14.** Comparison results between numerical FPCB and RPCB at a different orientation

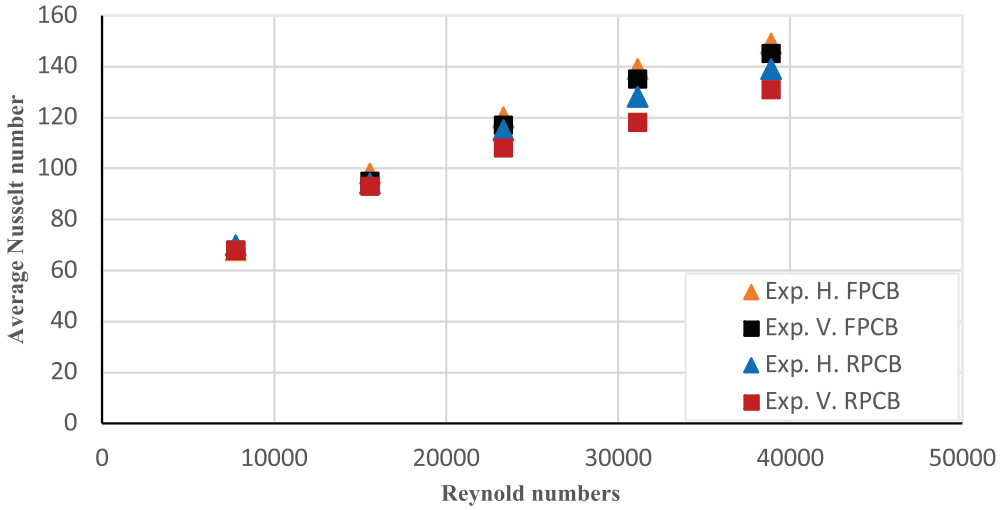


**Figure 15.** Comparison between experimental FPCB and RPCB at a different orientation

of air on the top surface of the board which forms eddies. It reduces the effect of forced convection. This behavior was determined by [33].

**Temperature contours and velocity vectors in the fluid domain**

This study was conducted using CFD simulation software, and the results showed good agreement with the experimental result. Through this study, it is possible to deduce three-dimensional diagrams of temperature and velocity, as shown in Figures (16), (17), (18) and (19) that illustrate the formation of the boundary layer and the effect of oscillation on heat transfer.

Figures 16 and 17 show the contours of the temperature distribution on the axis (YZ) on the CPU, with the effect of flow velocity on the shape of the boundary layer and the gradient of the temperature distribution. The difference between FPCB and RPCB can be seen in terms of the oscillation in the movement of the flexible board and the effect of this oscillation on the boundary layer that improves heat transfer. The effect of the buoyancy force generated on the CPU can be seen in Figure 17 in the vertical position as a result of the heat emitted from the source and the presence of obstacles in the path of the main current flow around the CPU, where the secondary currents reduce heat transfer from the vertical position compared to the horizontal position, velocity vectors and the influence of velocity on heat transmission can be shown in Figures 18 and 19. The difference between flexible and rigid boards can be noticed, with the flexible board behaving like a rigid board at a low

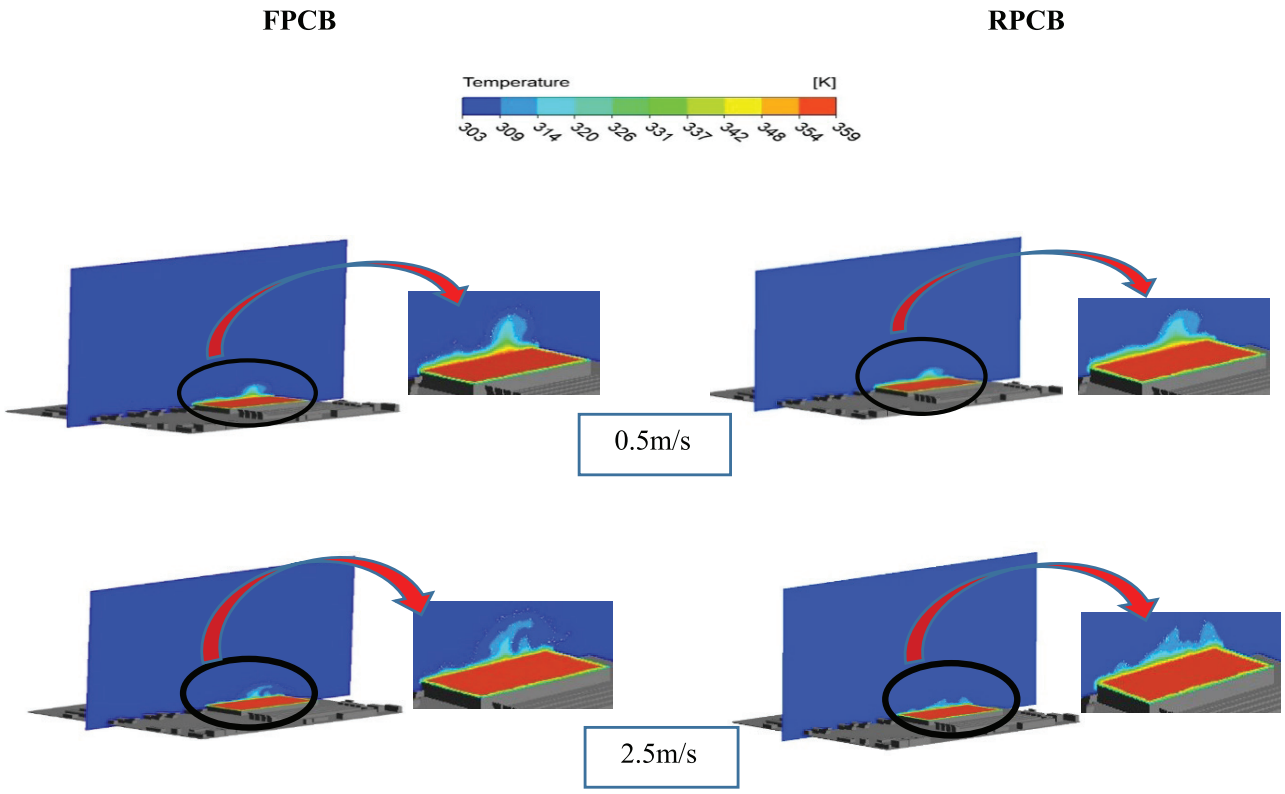


**Figure 16.** Temperature contours for horizontal FPCB and RPCB respectively at different inlet flow velocities

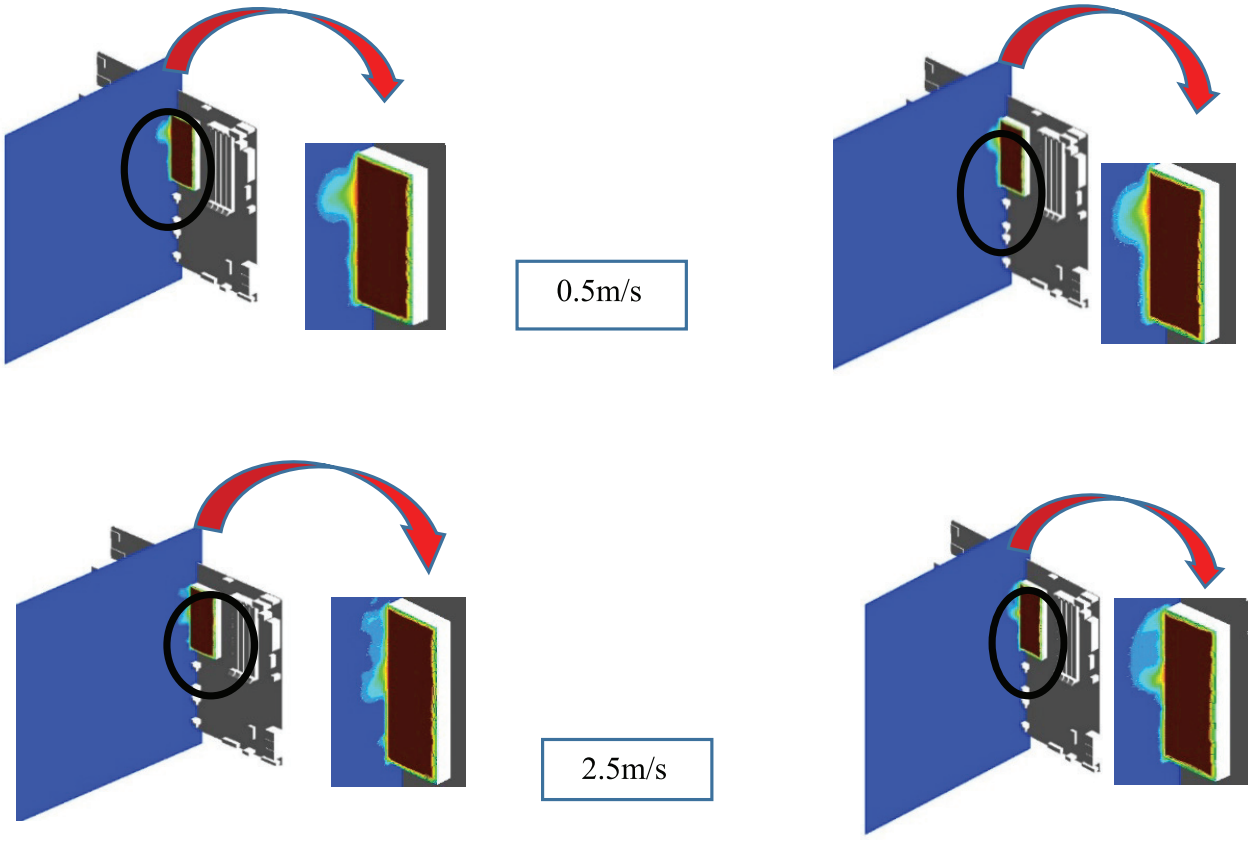


**Figure 17.** Temperature contours for vertical FPCB and RPCB respectively at different inlet flow velocities.

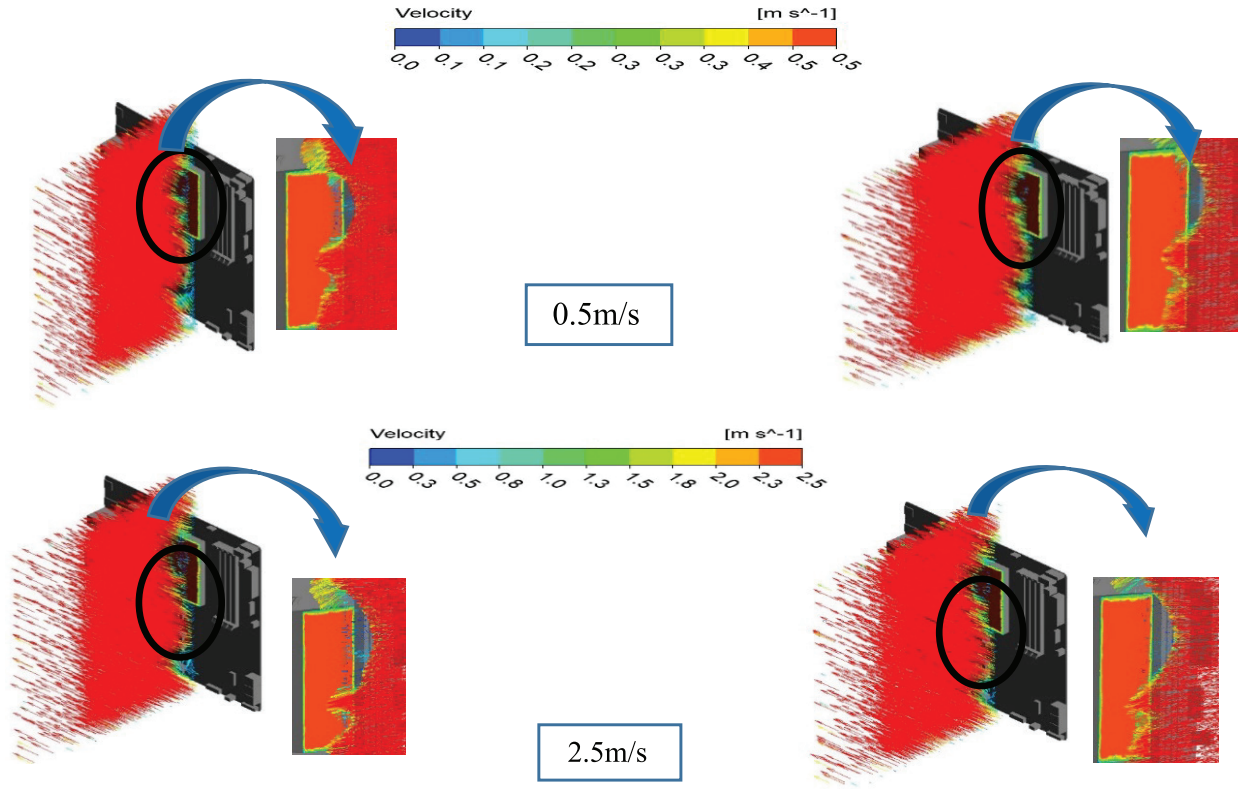


**Figure 19.** Velocity vectors for horizontal FPCB and RPCB respectively at different inlet flow velocities.

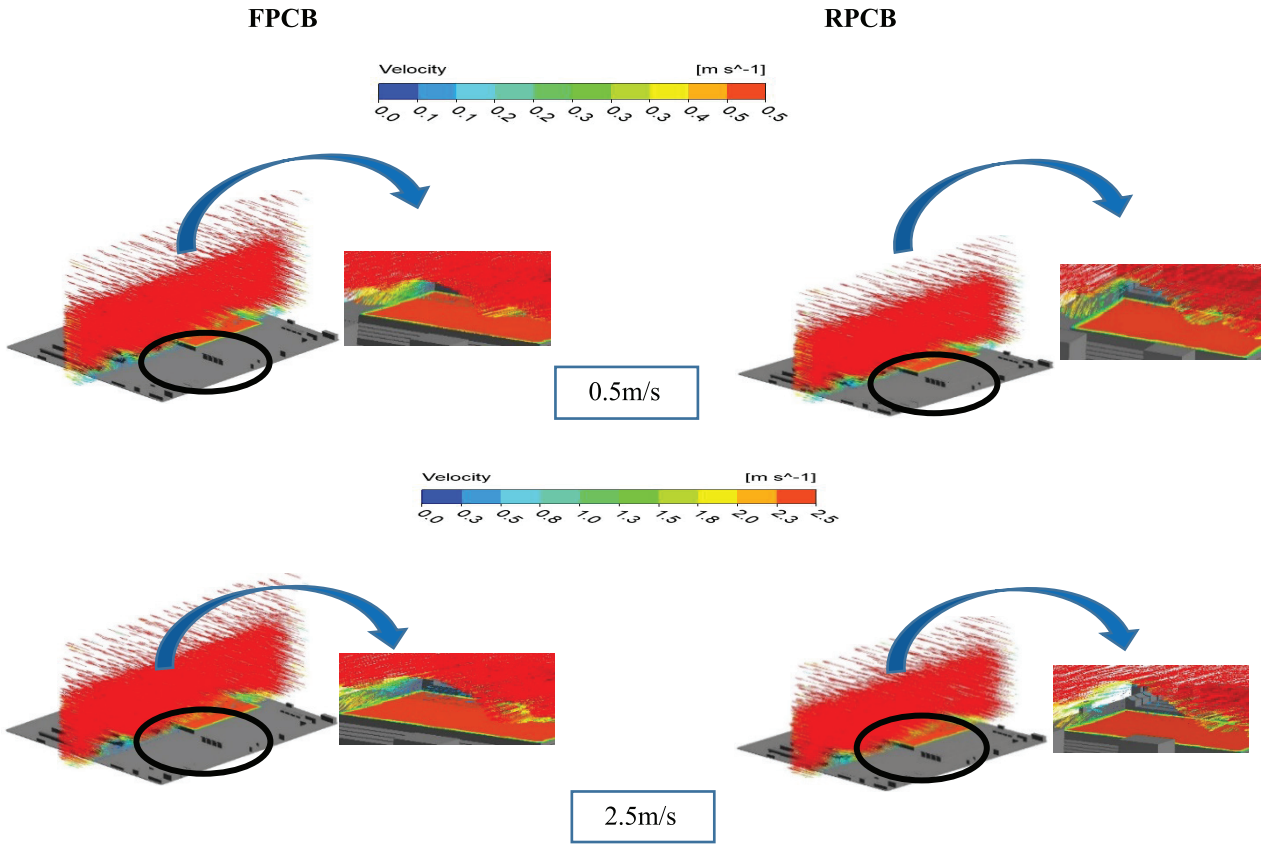


**Figure 18.** Velocity vectors for horizontal FPCB and RPCB respectively at different inlet flow velocities..

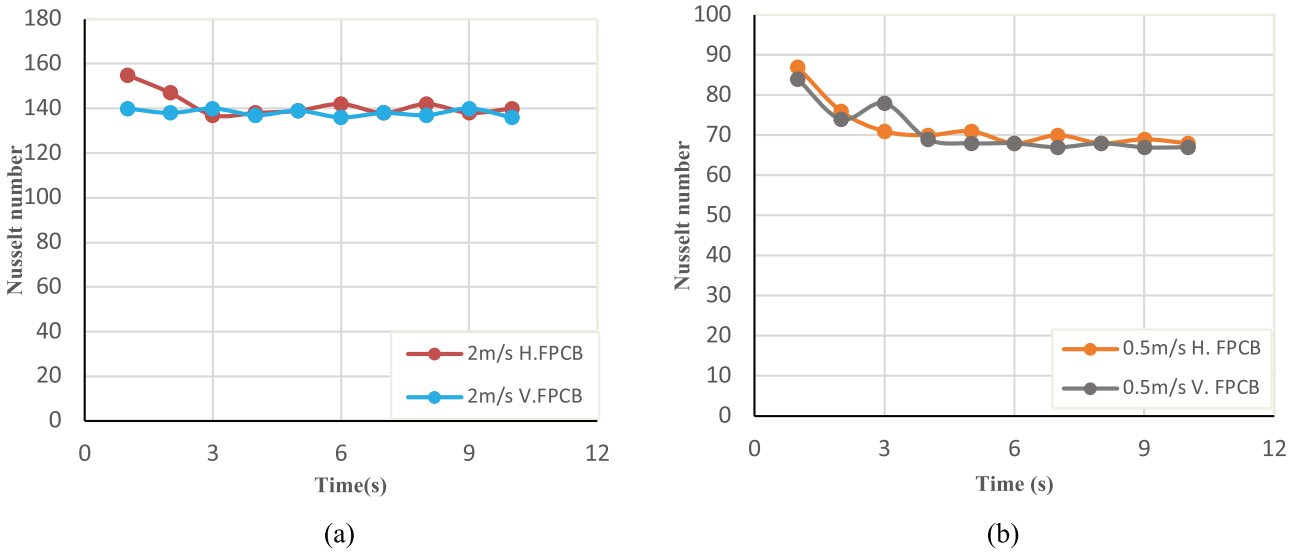


**Figure 20.** Variation of Nusselt number with time at different velocities.

speed of 0.5 m/s, with little interference and no effect on the boundary layer. However, as the airflow speed increases, heat transfer improves due to increased board fluctuation, resulting in a greater fracture in the boundary layers and increased heat transfer to the outside environment.

**Variations of Nusselt number with time**

The unstable distribution of the Nusselt number is shown in Figure 20. The figure shows the effect of fluctuation in the Nusselt number between high and low values, where the Nusselt number rise occurs for the boundary layer destroyed as a result of board fluctuation, and the average Nusselt number value decreases due to the temperature difference between the surface and the bulk fluid temperate.

**Friction Factor Effect on Printed Circuit Board**

The relationship between Reynold numbers and the friction factor can be seen in the figures (20 a and b), where it can be observed that friction decreases when Reynold numbers increase, and this is due to an increase in disturbances within the boundary layer. Figure 21 (a) shows the relationship between the friction factor and Reynold number in the flexible board, where it can be noted that the friction decreases when the Reynold numbers increases and the horizontal position is more than the vertical position

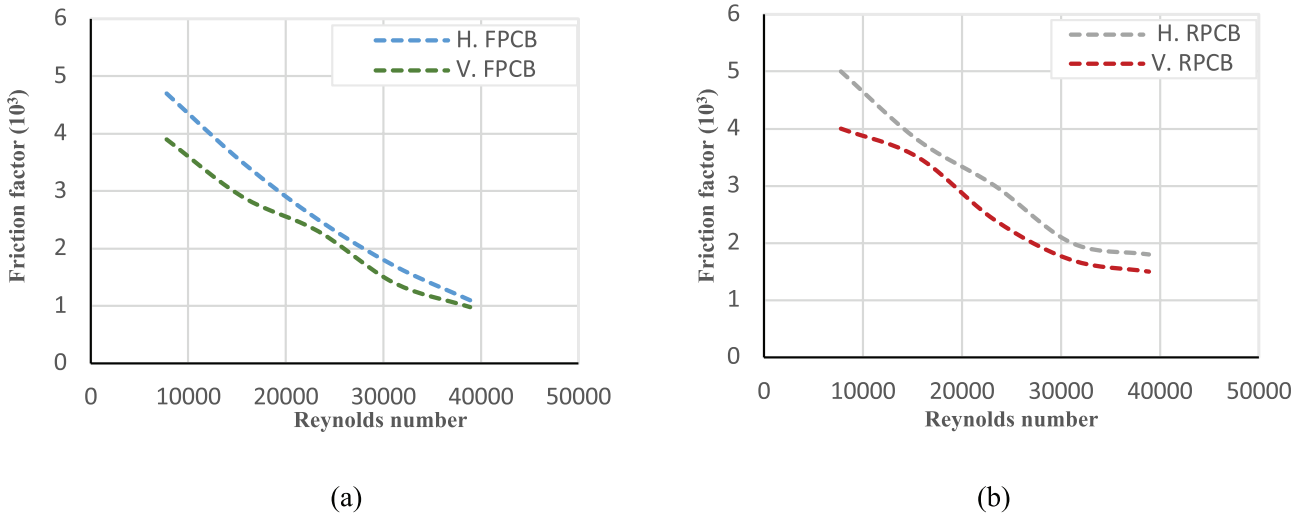


**Figure 21.** a) FPCB variation of numerical friction factor with Reynolds numbers at different orientations b) RPCB variation of numerical friction factor with Reynolds numbers at different orientations.

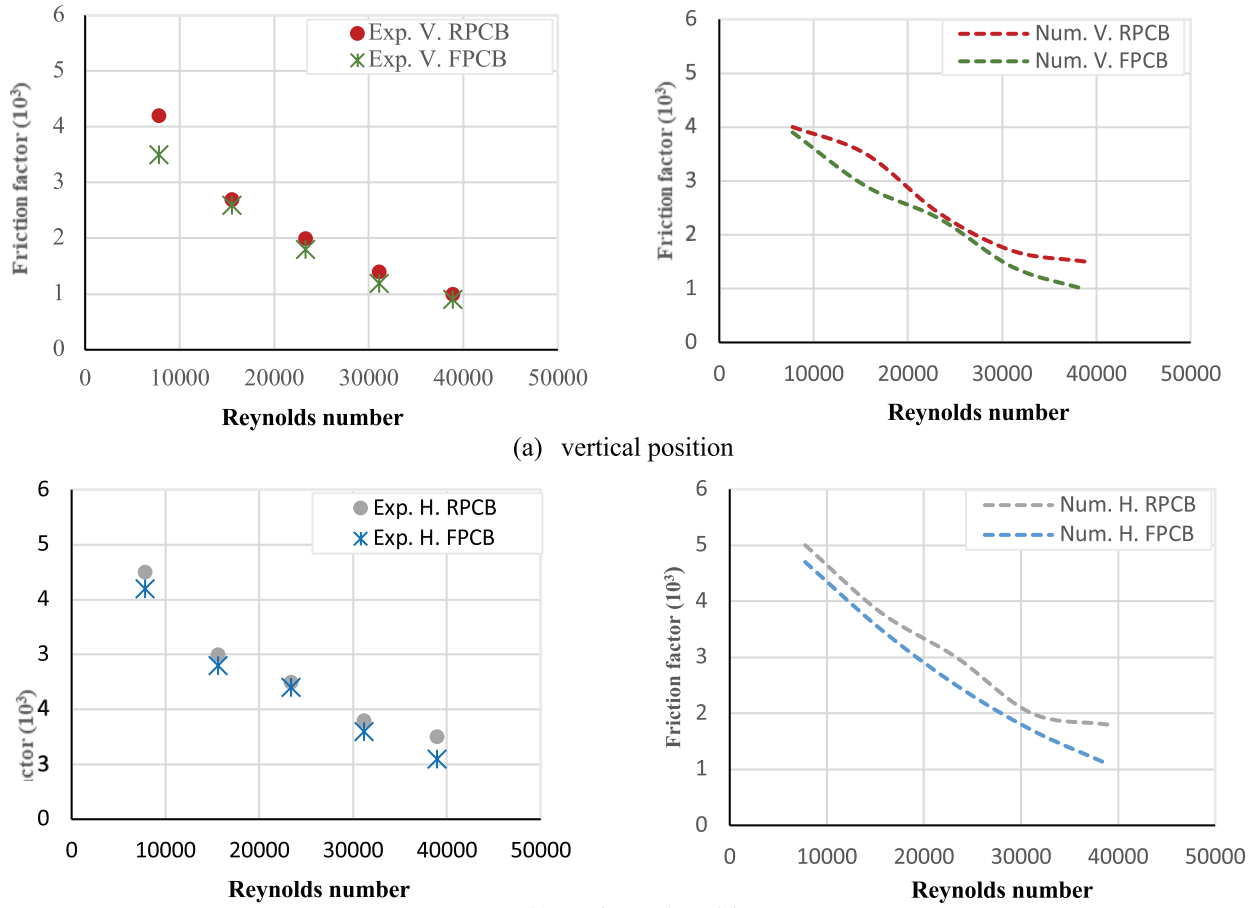


**Figure 22.** Comparison results between the RPCB and FPCB at the variation of friction factor with Reynolds number.

because of the acceleration in the flow near the wall under the influence of gravity.

The cohesive structure that exists in the turbulent boundary layer is primarily responsible for the friction force. Active interference of the turbulent boundary layer's coherent structure can effectively reduce friction force. Figure 22 reveals the comparison of friction factors in the rigid board and flexible board, where it can be seen that the friction in the flexible board is less than that in the rigid board as a result of the deflection on the board. The wall deforms and may interact with the turbulent boundary layer in order to reduce the friction factors added to the rapid changes in speed. Within the boundaries of the thermal boundary layers, as a result, vibration has a high ability to break the thermal boundary layers and hence reduce the friction. In general, an increase in inclination leads to an increase in the acceleration of the flow near the wall under the influence of gravity, and therefore higher friction occurs. The difference between the two horizontal positions and the vertical position can be observed. The reason for the difference is that the friction at low speed and in the horizontal position is more than that in the vertical position. This was also mentioned by [34, 35].

**Nusselt number correlation**

To find a relationship between Nu, Re, and Pe, correlation equations have been developed to study the heat transfer in RPCB and FPCB at the horizontal and vertical positions based on the results of the experiment.

A basic equation as follows relates to Nu, Re, and Pr. [36]

$$Nu = c\, Re^{m}\, Pr^{n} \quad (6)$$

In this study, Pr = 0.7 was fixed throughout the research, to get the values for c, m, and n, the values of the Reynold numbers and the Nusselt number were replaced into. Table 2 shows the values of c and the Exponent's m, n for each case.

**Table 2.** Constants of empirical equations

| Case study | c | m | n |
|---|---|---|---|
| V. RPCB | 2.6 | 0.34 | 0.3 |
| H. RPCB | 2.1 | 0.407 | 0.3 |
| V. FPCB | 1.45 | 0.446 | 0.3 |
| H. FPCB | 1.3 | 0.459 | 0.3 |

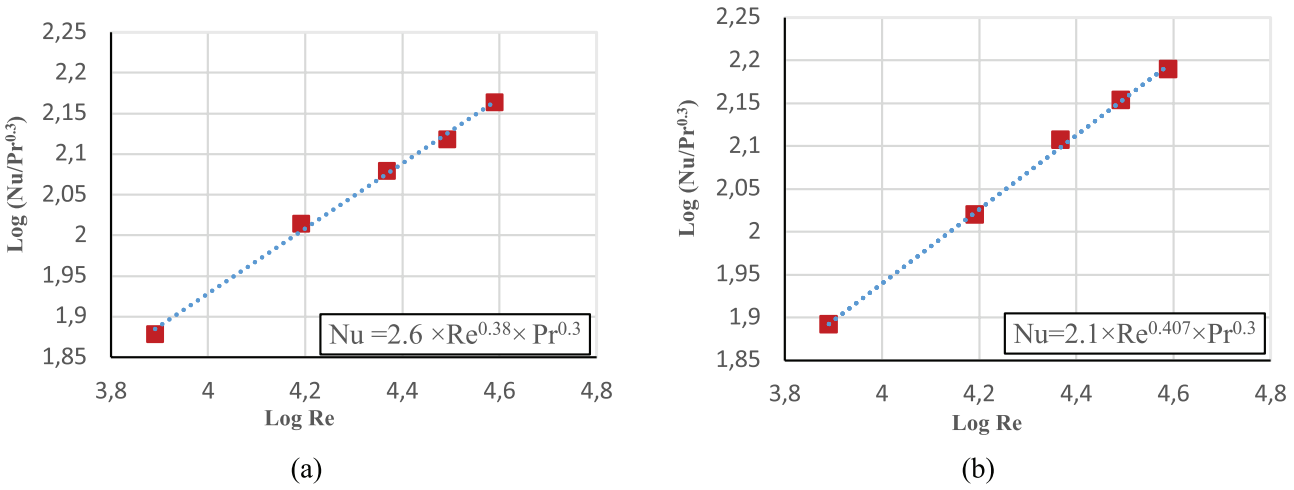


**Figure 23.** a) Vertical Logarithmic ($Nu/Pr^{0.3}$) versus logarithmic Reynolds numbers for RPCB b) Horizontal Logarithmic ($Nu/Pr^{0.3}$) versus logarithmic Reynold numbers for RPCB.

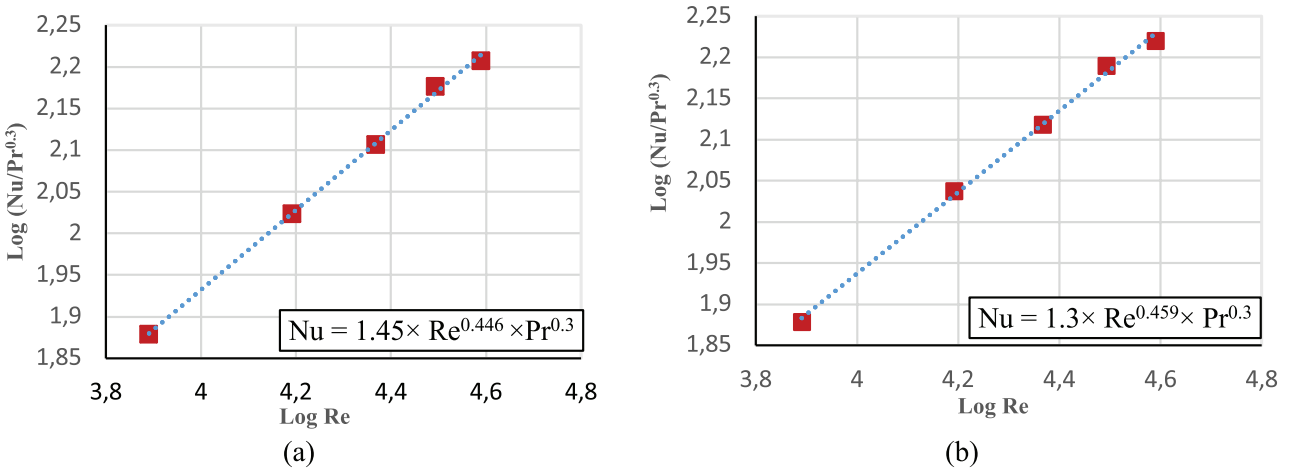


**Figure 24.** a) Vertical Logarithmic ($Nu/Pr^{0.3}$) versus logarithmic Reynold numbers for FPCB b) Horizontal Logarithmic ($Nu/Pr^{0.3}$) versus logarithmic Reynold numbers for FPCB.

Because the empirical correlation equations accurately captured the trend of the experimental results for each FPCB and RPCB, they had a low percentage of error of 1.76 percent. The current study's empirical equations are valid for (7000>Re>40000), as shown in Figures 23 and 24 [37].

## CONCLUSION

The improvement of heat transfer in electronic circuits with PCB investment has been studied numerically and experimentally. This enhancement is achieved by changing the direction of the board and studying the replacement of the rigid board with a flexible board to invest its properties in improving heat transfer. The result shows that after the comparison between the flexible board and rigid board, the heat transfer improvement rate of flexible board was 7.6% in the horizontal position and 7% in the vertical position. And the effect of motherboard orientation found that the Nusselt number in the horizontal position had better heat transfer performance than in the vertical position. The effect of friction on a flexible board vs a rigid board was investigated. Because of the deflection of the flexible board, the rigid board has around 38% higher friction than the flexible board in the horizontal position and 40% more in the vertical position. And the friction effect of the flexible board in the horizontal position is 18% more than in the vertical position, and the friction in the horizontal position of the rigid board is 17% from the vertical p.osition. General correlations of average Nusselt number for RPCB and FPCB in vertical and horizontal orientations as a function of Reynold and Prandtl numbers have been developed. In future studies, investigate the influence of board

geometry and electronic part distribution on the flexible board to obtain the optimal fluctuation to optimize heat transfer through the board.

## NOMENCLATURE

| | |
|---|---|
| $A$ | Surface area $m^2$ |
| $D$ | Diameterm |
| $h_{ave}$ | Average heat transfer coefficient $W/m^2.K$ |
| $I$ | Current A |
| $V$ | Voltage volt |
| $k$ | Thermal conductivity W/m.K |
| $l$ | Length m |
| $l_c$ | characteristic length m |
| $\dot{m}$ | Mass flow rate kg/s |
| $Nu_{ave}$ | Average Nusselt number …. |
| $Pr$ | Prandtl number …. |
| $Q$ | Total heat power of heater W |
| $Re$ | Reynold number …. |
| T | Temperature °C |
| $T_b$ | Bulk temperature °C |
| R | Result |
| S | uncertainty |
| X | variable data |
| $T_{in}$ | Air temperature at inlet °C |
| $T_{out}$ | Air temperature at outlet °C |
| $t$ | Time *sec* |
| $\Delta p$ | Pressure drop *Pa* |
| $u, v, w$ | Velocity component in Cartesian coordinate *m/s* |
| $c_p$ | Specific heat J/kg.K |

Abbreviation

| | |
|---|---|
| FPCB | Flexible printed circuit board |
| RPCB | Rigid printed circuit board |
| H.T | Heat transfer |
| B.L | Boundary layer |
| FVM | Finite Volume Method |
| BGA | Ball grid array |
| CFD | Computational fluid dynamics |
| H | Horizontal position |
| V | Vertical position |
| Exp. | Experimental result |
| Num. | Numerical result |
| CPU | Central Processing Unit |
| IC | Integrated Circuit |
| 3D | three-dimensional |

Greek Symbols

| | |
|---|---|
| $f$ | Friction factor …. |
| μ | Dynamic viscosity kg/m.s |
| $\kappa$ | Turbulent kinetic energy $m^2/s^2$ |
| $\rho$ | Density $kg/m^3$ |

## AUTHORSHIP CONTRIBUTIONS

Authors equally contributed to this work.

## DATA AVAILABILITY STATEMENT

The authors confirm that the data that supports the findings of this study are available within the article. Raw data that support the finding of this study are available from the corresponding author, upon reasonable request.

## CONFLICT OF INTEREST

The author declared no potential conflicts of interest with respect to the research, authorship, and/or publication of this article.

## ETHICS

There are no ethical issues with the publication of this manuscript.

## REFERENCES

[1] Ghasemi B, Aminossadati S. Numerical simulation of mixed convection in a rectangular enclosure with different numbers and arrangements of discrete heat sources. Arab J Sci Eng 2008;33:189−207.

[2] Anandakrishnan M, Balaji C. CFD Simulations of thermal and flow fields inside a desktop personal computer cabin with multi-core processors. Eng Appl Comput Fluid Mech 2009;2:277−288. [CrossRef]

[3] Wits WW, Vaneker THJ, Mannak JH, Legtenberg R. Novel cooling strategy for electronic packages: Directly injected cooling. CIRP J Manuf Sci Technol 2009;1:142−147. [CrossRef]

[4] Ilker Tari, Fidan Seza Yalcin. CFD analyses of a notebook computer thermal management system and a proposed passive cooling alternative. IEEE Trans Compon Packag Technol 2010;33:443−452. [CrossRef]

[5] Hotta TK, Venkateshan SP. Natural and mixed convection heat transfer cooling of discrete heat sources placed near the bottom on a PCB. World Acad Sci, Eng Technol, Int J Mech, Aerospace, Industrial, Mech Manuf Eng 2012;6:1446−1453.

[6] Leong WC, Abdullah MZ, Khor CY, Ong EES. Study on the Fluid-Structure interaction of flexible printed circuit board electronics in the flow environment. IEEE Trans Compon Packag Manuf Technol 2012;2:1335−1345. [CrossRef]

[7] Rout SK, Mishra DP, Thatoi DN, Acharya AK. Numerical analysis of mixed convection through an internally finned tube. Adv Mech Eng 2012;4:918342. [CrossRef]

[8] Nakla ME. Forced convection heat transfer in two-dimensional ribbed channels with varying heat flux profiles using ANSYS' software and modeling. Arab J Sci Eng 2014;39:2157−2164. [CrossRef]

[9] Hussein AK, Rout SK, Fathinia F, Chand R, Mohammed HA. Natural convection in a triangular top wall enclosure with a solid strip. J Eng Sci Technol 2015;10:1326−1341.

[10] Navas RKB, Vignan BVC, Durganadh M, Krishna CR. Analysis and optimization of central processing unit process parameters. IOP Conf Ser Mater Sci Eng 2017;197:012084. [CrossRef]
[11] Choudhary P, Pankaj SK, Tomar M, Thakur HC. Unsteady analysis of heated inclined fin-plate placed inside square enclosure. 2nd Int Conf Convergence Technol (I2CT) 2017. Available at: https://ieeexplore.ieee.org/document/8226220/authors#authors. Accessed Nov 16, 2023. [CrossRef]
[12] Lim CH, Abdullah MZ, Azid IA, Aziz MSA. Experimental and numerical investigation of flow and thermal effects on flexible printed circuit board. Microelectron Reliab 2017;72:5−17. [CrossRef]
[13] Yıldız S. Investigation of natural convection heat transfer at constant heat flux along a vertical and inclined plate. J Therm Eng 2018;4:2431−2444. [CrossRef]
[14] Nodooshan AA. Heat transfer and friction characteristics of an array of perforated fins under laminar forced convection. J Therm Eng 2019;5:115−122. [CrossRef]
[15] Mathew VK, Hotta TK. Experiment and numerical investigation on optimal distribution of discrete ICs for different orientation of substrate board. Int J Ambient Energy 2022;43:1607−1614. [CrossRef]
[16] Chen Y. Analysis and research on Thermal-Force coupling performance of a vehicle controller PCB board.2020 3rd International Conference on Electron Device and Mechanical Engineering (ICEDME). 2020. Available at: https://ieeexplore.ieee.org/document/9122139/authors#authors. Accessed Nov 16, 2023. [CrossRef]
[17] Aun SHA, Ghadhban SA, Jehhef KA. Experimental and numerical investigation of convection heat transfer in an enclosure with a vertical heated block and baffles. J Therm Eng 2021;7:367−386. [CrossRef]
[18] Durgam S. Forced convection from IC chips on printed circuit boards generating high heat fluxes. J Inst Eng (India): Ser C 2021;102:933−940. [CrossRef]
[19] Mehta K, Mehta N, Patel V. Experimental investigation of the thermal performance of closed loop flat plate oscillating heat pipe. Exp Heat Transf 2021;34:85−103. [CrossRef]
[20] Gupta SK, Kukreja N. Optimization of cooling fan speed for heat transfer enhancement of electronic chip using CFD. IOP Conf Ser: Mater Sci Eng 2021;1116:012107. [CrossRef]
[21] Nadezhda Evstatieva, Boris Evstatiev. Modelling the temperature conditions of a printed circuit board. 12th Int Symp Adv Topics Elect Eng (ATEE) 2021. Available at: https://www.masader.om/eds/detail?db=edseee&an=edseee.9425281&isbn=9781665418775. Accessed Nov 16, 2023. [CrossRef]
[22] Bilawane RR, Mandavgade NK, Kalbande VN, Patle LJ, Kanojiya MT, Khorgade RD. Experimental investigation of natural convection heat transfer coefficient for roughed inclined plate. Mater Today: Proc 2021;46:7926−7931. [CrossRef]
[23] Kadum M, Imran AA, Aljabair S. Heat transfer in electronic systems printed circuit board: A review. Eng Technol J 2022;40:99−108. [CrossRef]
[24] Dash B, Nanda J, Rout SK. The role of microchannel geometry selection on heat transfer enhancement in heat sinks: A review. Heat Transfer 2022;51:1406−1424. [CrossRef]
[25] CFD Experts. ANSYS Fluent Theory Guide; Ansys. Inc.: Canonsburg, PA, USA. Available at: https://dl.cfdexperts.net/cfd_resources/Ansys_Documentation/Fluent/Ansys_Fluent_Theory_Guide.pdf. Accessed Nov 16, 2023.
[26] http://ftp.demec.ufpr.br/disciplinas/TM702/Versteeg_Malalasekera_2ed.pdf
[27] Intel. Intel® Core™ i9 processors. Available at: https://www.intel.com/content/www/us/en/products/details/processors/core/i9/products.html. Accessed Nov 16, 2023.
[28] Ismaeel TA, Aljabair S, Abdulrazzaq OA, Abood YA. Energy recovery of moving vehicles' wakes in highways by vertical axis wind turbines. FME Trans 2020;48:557−565. [CrossRef]
[29] Venkateshan SP. Mechanical measurements. New York: John Wiley & Sons; 2015. Available at: https://onlinelibrary.wiley.com/doi/book/10.1002/9781119115571. Accessed Nov 16, 2023. [CrossRef]
[30] Kadum ME, Aljabair S, Imran AA. Experimental and numerical study heat transfer performance for printed circuit board. AIP Conf Proc 2023;2830:070003. [CrossRef]
[31] Wang B-F, Zhou Q, Sun C. Vibration-induced boundary-layer destabilization achieves massive heat-transport enhancement. Sci Adv 2020;6:1−6. [CrossRef]
[32] Sarhan AR, Karim MR, Kadhim ZK, Naser J. Experimental investigation on the effect of vertical vibration on thermal performances of rectangular flat plate. Exp Therm Fluid Sci 2019;101:231−240. [CrossRef]
[33] Leung CW, Kang HJ. Convective heat transfer from simulated air-cooled printed-circuit board assembly on horizontal or vertical orientation. Int Commun Heat Mass Transf 1998;25:67−80. [CrossRef]
[34] Li W, Roggenkamp D, Hecken T, Jessen W, Klaas M, Schröder W. Parametric investigation of friction drag reduction in turbulent flow over a flexible wall undergoing spanwise transversal traveling waves. Exp Fluids 2018;59:1−18. [CrossRef]
[35] Zhang L, Shan X, Xie T. Active control for wall drag reduction: Methods, mechanisms and performance. IEEE Access 2020;8:7039−7057. [CrossRef]
[36] Çengel YA. Heat transfer: A practical approach. New Yırk: McGraw-Hill series in mechanical Engineering; 2004.
[37] Al-Jabair SJH, AL-Taee AAHA. Experimental study of heat transfer coefficients of shell and helically coiled tube heat exchangers. Eng Technol J 2013;31:172−196. [CrossRef]